



Adsorption of non-steroidal anti-inflammatory drugs (diclofenac and ibuprofen) from aqueous medium onto activated onion skin

Ghulam Abbas^a, Iqbal Javed^a, Munawar Iqbal^{b,*}, Rizwan Haider^c, Fida Hussain^{d,e,f,g}, Naseem Qureshi^h

^aDepartment of Chemistry, University of Agriculture, Faisalabad 38000, Pakistan

^bDepartment of Chemistry, The University of Lahore, Lahore, Pakistan, email: bosalvee@yahoo.com (M. Iqbal)

^cDepartment of Chemistry, Quaid-i-Azam University, Islamabad, Pakistan

^dDepartment of Botany, Qurtuba University of Science and Information Technology, Peshawar 25100, KPK, Pakistan

^eSchool of Resources, Environmental & Chemical Engineering, Nanchang University, Nanchang 330000, China

^fKey Laboratory of Poyang Lake Environment and Resource Utilization, Nanchang University, Nanchang 330000, China

^gDepartment of Botany, Islamia College, Peshawar 25100, Pakistan

^hDepartment of Chemistry, Karakoram International University, Gilgit 15100, Pakistan

Received 28 December 2016; Accepted 10 September 2017

ABSTRACT

Diclofenac (DCF) and ibuprofen (IBP) adsorption onto acids (HCl, H₂SO₄ and H₃PO₄) pre-treated onion skin (OS) was studied as a function of pH, adsorbent dosage, drugs initial concentrations and contact time. The H₂SO₄-OS (adsorbent) showed higher drugs adsorption efficiency followed by H₃PO₄-OS and HCl-OS and NAT-OS (native). The drugs loaded and un-loaded OS were characterized by energy dispersive X-ray and scanning electron microscope techniques, which revealed a considerable change in OS composition and changed surface morphology. Pseudo-second-order kinetic model fitted well to both the drugs adsorption data. Freundlich isotherm explained well the drugs adsorption onto OS adsorbents. The optimum conditions of pH, adsorbent dosage and contact time were 6.5, 0.05 mg/g and 220 min, respectively. At optimum condition, the DCF and IBP adsorptions were 134.003 and 91.99 mg/g, respectively, which were 81.90% and 65.99% removal of the initial concentrations. Results revealed that OS pre-treated with mineral acids is a potential adsorbent and could possibly be used for the remediation of drugs wastewater.

Keywords: Onion skin; Mineral acid pre-treatments; Anti-inflammatory drugs; Surface morphology; Elemental composition

1. Introduction

Recently, pharmaceutical agents have gained attention due to their toxic nature. The drugs have prime importance for the therapeutic treatment of diseases, but on entrance into the environment these may harm the non-targeted species [1]. Since pharmaceutical agents are harmful at very low concentration [2] and long-term exposure can affect living organisms adversely [3]. Un-controlled discharge of pharmaceutical agents may reach even ground water and pollute the drinking

water sources [4]. Non-steroidal anti-inflammatory drugs (NSAIDs) are one of the most consumed classes of pharmaceuticals with several tons annual production [5]. Diclofenac (2-[(2,6-dichlorophenyl)amino] benzene acetic acid) (chemical formula C₁₄H₁₀Cl₂NO₂, MW 296.16 g/mol) is extensively consumed and it is a persisting contaminate and has been reported in drinking water [6] up to 15 µg/L [7]. DCF exposure may cause detrimental effects, such as hemodynamic changes or thyroid tumors [8]. DCF is responsible for the decline of vulture (*Gyps bengalensis*) species in Pakistan, India, Bangladesh and southern Nepal. This decline was started in 1990 in India and more than 95% of *Gyps bengalensis* species

* Corresponding author.

declined due to DCF [9]. Ibuprofen [2-(4-(2-methyl propyl) phenyl)-propionic acid (molecular formula $C_{13}H_{18}O_2$, MW 206.3 g/mol) is also NSAID, which is also detected in wastewater at elevated concentration [10]. So far, there is need to remove the drugs from wastewater and different techniques have been used for the remediation of pollutants [11–15], that is, coagulation and sedimentation [16], biodegradation [17], phototransformation [18], ozonation [19] and sonolysis and ultrasonication [20]. The non-destructive treatment methods transform drugs into by-products, which might also be toxic [21,22]. Adsorption process is considered a better for water treatment due to several advantages and under the current scenario of environmental pollution [23–53], there is a need to explore the cost-effective adsorbents from natural resource [54–58].

In Pakistan, onion is commercially grown on an area of 131.4 thousand hectares with annual production of 1.8 million tons. The onion growing areas include Kasur and Vehari (Punjab), Mirpurkhas, Hyderabad, Noushahro Feroze, Nawabshah, Badin, Sanghar, Dadu, Ghotki and Shikarpur (Sindh), Swat and Dir (KPK) and Kharan, Chaghi, Mastung, Kalat, Nasirabad, Killa Khuzdar, Turbat, Saifullah and Jaffarabad (Balochistan) [59]. The total world production of onion is ~86.34 million tons and Pakistan is on 8th position with 2.25% including China (28.68%), India (18.45%), USA (3.89%), Iran (2.90%), Egypt (2.66), Turkey (2.48%) and Russia (2.46%) of total world onion production. The onions are used in pickling, chutney and sauces preparation [59,60] and as a result of onion processing, a huge amount of OS is produced (Fig. 1). So far, the OS waste could possibly be used as adsorbent. Previously, cold plasma-treated and formaldehyde-treated onion skins (OSs) were used as an adsorbent for the adsorption of methylene blue dye and authors revealed that adsorption capacities of methylene blue onto onion were 90.94% and 95.54% onto cold plasma-treated and formaldehyde-treated OSs [61].

Therefore, in present investigation OS waste was investigated as an adsorbent for the adsorption of DCF and ibuprofen (IBP) drugs. The OS was modified by treating with mineral acids and employed for the adsorption of DCF and IBP drugs. The loaded and un-loaded OS adsorbents were



Fig. 1. Onion (A) in field, (B) raw onion and (C) onion skin waste produced during onion processing.

characterized by scanning electron microscope (SEM) and energy dispersive X-ray (EDX) techniques.

2. Material and methods

2.1. Reagents and chemicals

Diclofenac (DCF) sodium (MW 318.1 g/mol, chemical formula = $C_{14}H_{10}Cl_2NNaO_2$, pKa = 4.2, $\log K_{ow} = 0.57$) and IBP (MW 206.3 g/mol, chemical formula = $C_{13}H_{18}O_2$) were purchased from SAMI pharmaceutical company (Pakistan). NaOH (97%), HCl (36%), H_2SO_4 (96%), H_3PO_4 (85%), ethanol (95%) and methanol (99.85%) were purchased from Sigma-Aldrich (Germany). For the preparation of solutions, ultra-pure water (Millipore system) was used.

2.2. Biomass collection and preparation

The OS waste was collected from hostel canteens, University of Agriculture, Faisalabad. Collected biomass was washed with water, dried in open air and ground in a grinder to fine powder and passed through seiver (OCT-DIGITAL-4527-01). The particle of 0.25 mm size was collected and subjected to mineral acid pre-treatments (1 M HCl, H_2SO_4 and H_3PO_4 solutions) separately. After acidic pre-treatment, the masses were washed with distilled water (four to five times). Then, the biomass was dried in oven at 50°C overnight, ground and fine powder was stored in airtight glass bottle and used for the adsorption of DCF and IBP drugs (Fig. 2).

2.3. Adsorption procedure

The adoption experiments were conducted in 250 mL Erlenmeyer flask with constant shaking (120 rpm, PA 250/25.H shaker) at room temperature. The drugs initial concentration, contact time, adsorbent dose and pH were studied in the range of 10–200 mg/L; 10–1,400 min; 0.05–0.30 g and 2.5–8.5, respectively. HCl/NaOH (0.1 M) solution was used for pH adjustment. To perform the adsorption of DCF and IBP onto OS adsorbents, a 100 mL solution of each drug was mixed with adsorbent in conical flasks and covered with aluminum foil. The flasks were placed on a rotating shaker at 120 rpm at room temperature. After stipulated time period, the flasks were removed and adsorbent was separated from solution by centrifugation, and DCF and IBP residual concentration was estimated spectrophotometrically at 276 and 224 nm, respectively. The adsorption capacities and percentage removal of drugs were estimated using relations shown in Eqs. (1) and (2), respectively [62]:

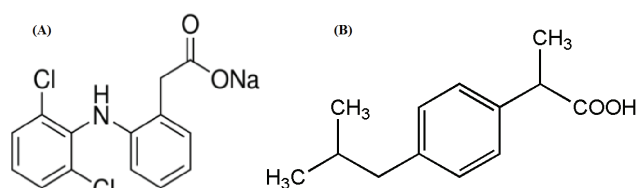


Fig. 2. Structures of (A) diclofenac and (B) ibuprofen.

$$q_e = \frac{(C_i - C_f) \frac{V}{100}}{m} \quad (1)$$

$$R(\%) = \left[\frac{C_i - C_f}{C_i} \right] \times 100 \quad (2)$$

where q_e is adsorption capacity, R (%) is percentage recovery, C_i and C_f are the initial concentration and concentration at time t of drugs, V is the volume of solution (mL) and m is the adsorbent dose (g).

2.4. SEM and EDX analysis

The loaded and un-loaded OS adsorbents were analyzed by SEM (JEOL, JSM-6400, Japan) and EDX techniques for surface morphology monitoring and elemental analysis, respectively [63].

2.5. Statistical analysis

All the adsorption experiments were performed in triplicate and data thus obtained was averaged and reported as mean \pm SD (the SD values for all adsorption experiments were in the range of 2%–4%). The regression coefficient (R^2) values of isotherms and kinetic models were determined using statistical functions of Microsoft Excel, 2007 (version Office XP, Microsoft Corporation, USA).

3. Results and discussion

3.1. Effect of pH

pH of the medium affects the activity of the adsorbent surface and ions in the medium by affecting the functional groups on adsorbent surface and solution chemistry [27]. The effect of pH for the adsorption of DCF and IBP onto OS was studied in the pH range of 2.5–8.5 and responses are shown in Figs. 3(A) and (B). Initially, the adsorption of both drugs increased by increasing pH up to 6.5 and then, decreased at higher pH. The pH of the zero charge point (pH_{pzc}) of OS is 6.61–6.64 [54], so the low adsorption of drugs at low pH was due to the extremely low solubility. The surface of OS carries net positive charge below pH_{pzc} and beyond the pH_{pzc} the surface carries a net negative charge. The acid dissociation constants (pK_a) of DCF and IBP are 4.21 and 4.4 [64]. This implies that drugs molecule carries negative charge for $\text{pH} < \text{pK}_a$ and exists in protonated form and so on. Therefore, under this condition, both adsorbent surface and adsorbate carry positive charge and repulsion hindered the adsorption of both DCF and IBP (Eqs. (3)–(5)). Under basic pH, the dissociation of the functional groups on the adsorbent surface and drugs also exists in protonated form (Eqs. (6)–(8)), which results in repulsion between drug ions and adsorbent surface. The optimal pH for both drugs was 6.5–7.0. Previously, acidic drugs also showed similar adsorption behavior as a function of pH [65–67], that is, the adsorption of a complex mixture of 12 selected pharmaceuticals onto trimethylsilylated mesoporous SBA-15 was investigated. Solution pH

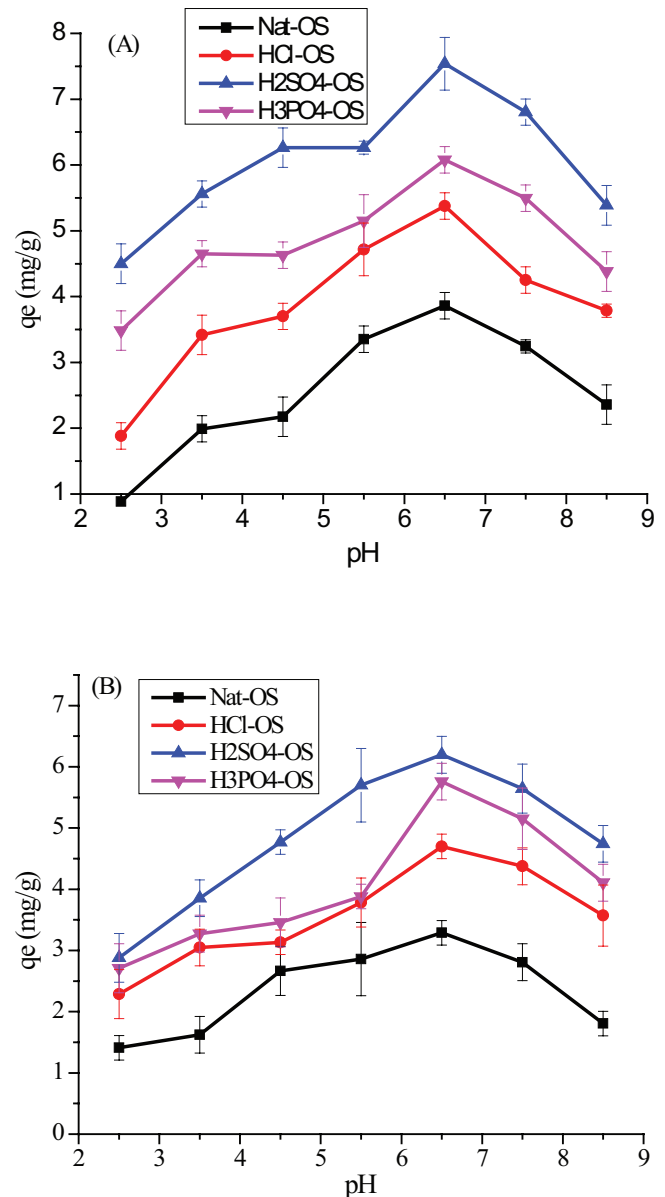
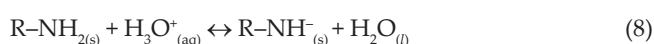
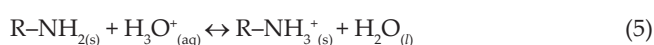
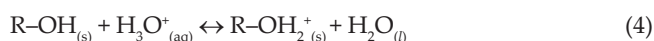


Fig. 3. Effect of pH on the adsorption of (A) diclofenac (B) ibuprofen on onion skin activated with acids (adsorbent dose = 0.05 g, pH = 2.5–8.5, contact time = 4 h, initial concentration of drugs = 20 mg/L).

significantly affected the adsorption of agents onto SBA-15 [66]. In another study, bagasse adsorption efficiency for DCF has been reported and adsorption was significantly higher under slight acidic condition [66]. Similarly, the adsorptions behavior of IBP, ketoprofen, naproxen and DCF onto activated carbon adsorbent was also in line with present investigation [67]. Waste-derived activated carbon also showed similar behavior for the adsorption of IBP as a function of pH and at pH 6.5, the drug was in anionic form and adsorbent surface was in protonated form due to acid pre-treatments and resultantly, the adsorption was enhanced due to electrostatic attraction between adsorbent and adsorbate.





3.2. Effect of adsorbent dose

The adsorbents doses effect was studied in the range of 0.05 to 0.30 mg/100 mL of solution and results are shown in Figs. 4(A) and (B). Both drugs showed higher adsorption at lower adsorbents doses. The adsorptions of DCF were recorded to be 10, 12, 14 and 12.5 (mg/g) for Nat-OS, HCl-OS, H₂SO₄-OS and H₃PO₄-OS, respectively, at 0.05 mg dose and these values reduced to 4, 5, 7 and 6 (mg/g) at 0.30 mg adsorbent dose. In case of IBP, the adsorption capacities were 9, 10, 11 and 10.5 (mg/g) for Nat-OS, HCl-OS, H₂SO₄-OS and H₃PO₄-OS, respectively, at 0.05 mg adsorbent, whereas these values reduced to 4, 5.5, 7 and 6 mg, respectively, when 0.30 adsorbent dose was used of Nat-OS, HCl-OS, H₂SO₄-OS and H₃PO₄-OS, respectively. Maximum adsorptions of drugs were achieved using 0.05 g adsorbent doses of Nat-OS, HCl-OS, H₂SO₄-OS and H₃PO₄-OS. The lower adsorption at higher adsorbent doses might be due to low surface area and availability of binding sites [26,27,68,69]. At higher adsorbent dose, constant drug concentration and solution volume might cause aggregation of adsorbent particles and resultantly, surface area was decreased [23,25,70–72]. The electrostatic interactions and overlapping or aggregation of adsorbent may block the active binding sites [73,74]. Similar adsorption behavior has also been reported previously for the adsorption of different adsorbates at different adsorbent doses [23–27,69,75–78].

3.3. Effect of initial drugs concentration

The sorption characteristics indicate that the surface saturation is dependent on the initial concentrations of the adsorbate. The effect of initial drugs concentrations were studied in the range of 10, 20, 30, 50, 100 and 200 mg/L and results thus obtained are shown in Figs. 5(A) and (B). The amounts of DCF and IBP adsorbed per unit mass of adsorbents increased with concentration, but the percentage removal decreased at higher concentration. In case of H₂SO₄-OS, the DCF percentage removal was 81.90% for initial concentration of 10 mg/L and this percentage decreased as the initial drug concentration increased to 100 mg/L at constant adsorbent dose. However, the adsorption capacity (*q*) increased from 8.88 to 87.17 (mg/g) when initial concentration increased from 10 to 100 mg/L of drug. Overall, the adsorption capacities of OS adsorbents were recorded in the following order: H₂SO₄-OS > H₃PO₄-OS > HCl-OS > Nat-OS. At lower drug concentration, the binding sites were available and then, by increasing the initial concentration, the competition between adsorbate and binding sites increased and resultantly, adsorption capacity decreased [25–27,69]. The initial

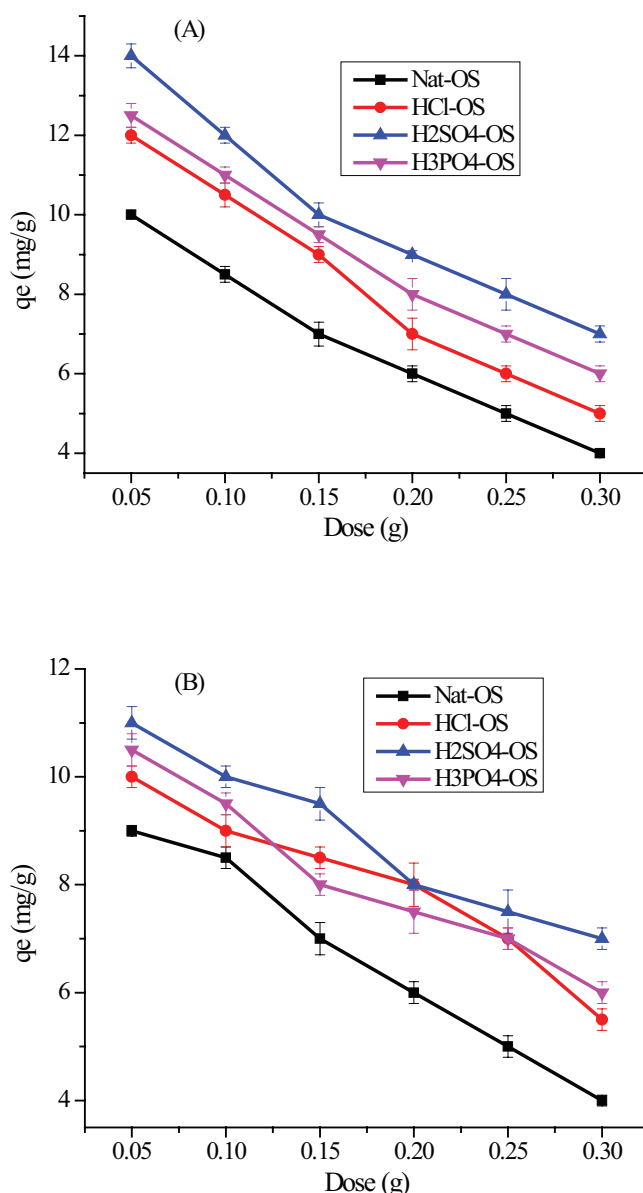


Fig. 4. Effect of adsorbent dose on the adsorption of (a) diclofenac (b) ibuprofen on onion skin activated with acids (adsorbent dose = 0.05–0.30 g, pH = 6.5, contact time = 4 h, initial concentration of drugs = 20 mg/L).

rate for the adsorption of drugs onto OS was higher, which was possibly due to the driving force (electrostatic forces) between adsorbate and binding sites [79]. Previous studies also revealed that at adsorbate concentration has significant effect on adsorption due to saturation of binding sites at higher initial concentration of adsorbate [23,24,62,72,75].

3.4. Effect of contact time

The effect of contact time for the adsorption of DCF and IBP was studied up to 1,400 min and results are shown in Figs. 6(A) and (B). Initially, the drug adsorption increased rapidly, slowed down and then became stable. The equilibrium was reached within 4 h for both drugs. The adsorption

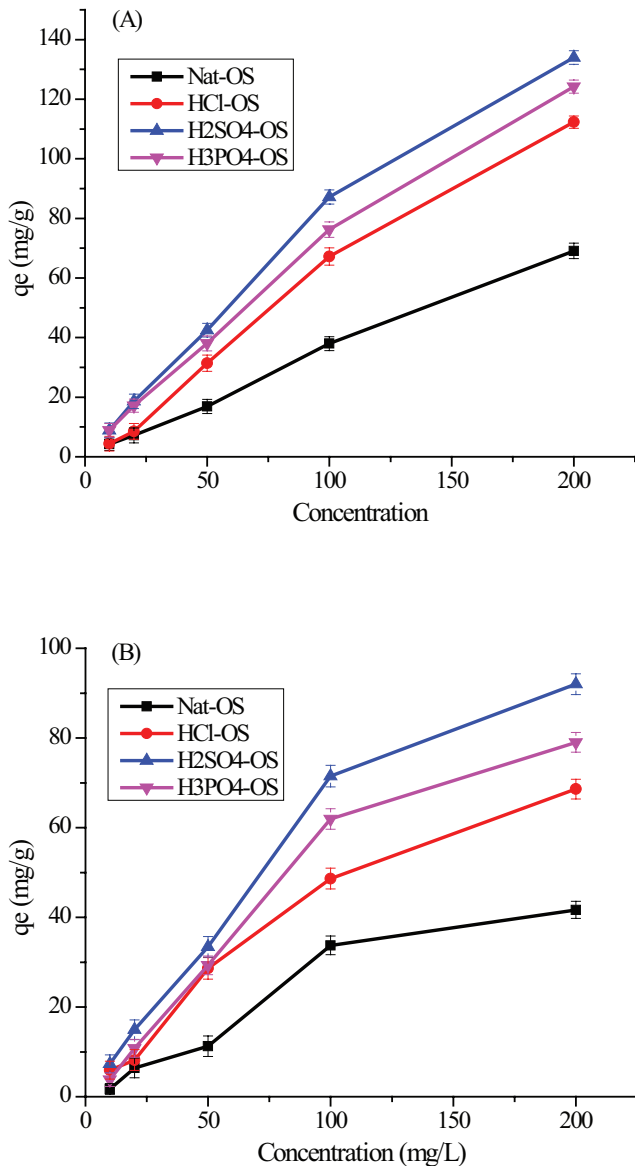


Fig. 5. Effect of initial drugs concentration on adsorption of (a) diclofenac (b) ibuprofen on onion skin activated with acids (adsorbent dose = 0.05 g, pH = 6.5, contact time = 4 h, initial concentration of drugs = 10–200 mg/L).

of drugs onto OS adsorbents took place in two phases. Initial fast phase (up to 30 min) followed by the slower second phase, which continued until the equilibrium was reached within 4 h and beyond this time the adsorption did not change. The initial rapid sorption was due to extracellular binding sites and on saturation of these sites, the adsorption process was slowed down due to intraparticle diffusion [25,27,62,69]. H₂SO₄-OS showed adsorption capacity of 72.3 mg/g (DCF) and 48.26 mg/g (IBP) followed by H₃PO₄-OS, HCl-OS and Nat-OS at equilibrium. The slow adsorption at later stages was due to intraparticle diffusion process dominating over adsorption [24,62,64,72,77,78]. The slow adsorption rate at latter stage can also be correlated with the difficulty faced by ions to occupy the remaining vacant binding sites [76]. Similar finding has also been reported previously for different adsorbents that

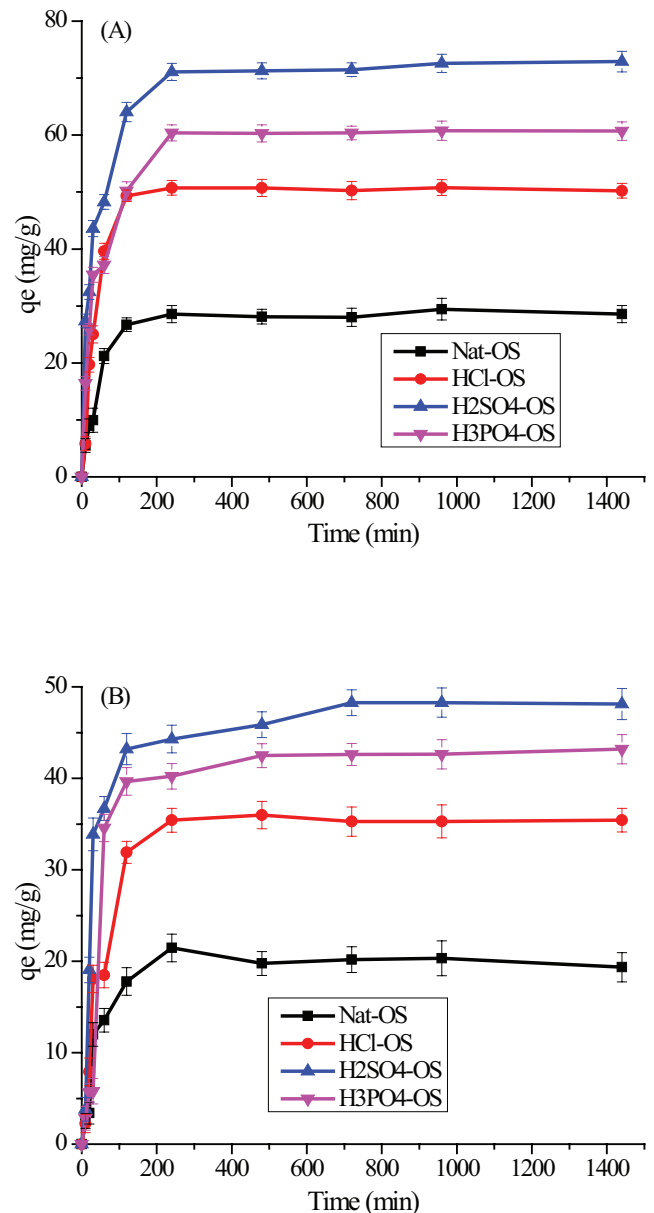


Fig. 6. Effect of contact time on the absorption of (a) diclofenac (b) ibuprofen on onion skin activated with acids (adsorbent dose = 0.5 g, pH = 6.5, contact time = 10–1,400 min, initial concentration of drug = 20 mg/L).

initially adsorption was very fast, slowed down and finally ceased, that is, pistachio hull [80], *Rosa damascena* [81], *Chlorella* species [82], *Ocimum americanum* seeds [83], *Aspergillus niger* NUA101 [84], banana peel [85], *Citrus cinensis* [86], walnut hull [87], *Phanerochaete cryosporium* [88] and *Mangifera indica* [24] and biocomposite [24–26,89] showed similar adsorption as a function of contact time.

3.5. Effect of mineral acid pre-treatments

The OS biomass was pre-treated with different acids (HCl, H₂SO₄ and H₃PO₄) and adsorption capacities were compared with Nat-OS in order to evaluate the effects of pre-treatments

with acids. Results revealed that the drugs adsorption increased significantly in response to acid pre-treatments (Fig. 7). The enhanced drugs adsorption might be due to modification of OS surface and exposure of binding sites. Moreover, elimination of impurities from adsorbent surface has also been reported due to acid pre-treatment [63,90]. The target compound is bonded with chemical moieties such as carboxyl ($-\text{COOH}$), amino ($-\text{NH}_2$), or phenol ($-\text{OH}$), so far, the chemical treatments may enhance the surface activity of adsorbent. By acid treatment, the metal ions and impurities are dissolved and active sites are appeared on the surface, which increased the adsorption capacity [91,92]. Among acids, H_2SO_4 showed maximum adsorption capacities of both drugs followed by H_3PO_4 and HCl . The acids have ability to dissolve the minerals and resultantly more ions can be transferred to the adsorbent surface. The functional groups are protonated by an acid treatment, adsorbent surface is modified and resultantly, adsorption capacity might affect. Cellulosic biomass have functional groups such as $-\text{COOH}$, $-\text{OH}$ and $-\text{NH}_2$, and on mineral acid pre-treatments, a positive charge is enhanced, which can attract the anionic species in the solution more efficiently [24,26,27,92]. The DCF adsorptions of 56.45%, 50.21% and 43.53% were recorded for H_2SO_4 , H_3PO_4 and HCl , respectively, and in case of IBP, the adsorption capacities were 52.8%, 45.52% and 30.64%, respectively. Previous studies also revealed that the adsorption capacity of adsorbent may increase as a result of surface modification by chemical treatment [92,93]. It is reported that the acidic pre-treatment of adsorbent changes the physico-chemical properties, that is, surface area change, modification of surface and pore volume. Moreover, pre-treatment also affects ions exchange capacity due to change in the surface chemistry of the adsorbent [94]. So far, the changes as a result of pre-treatments may change the adsorption characteristics and resultantly, the adsorption capacities were different for different acidic treatments of OS biomass.

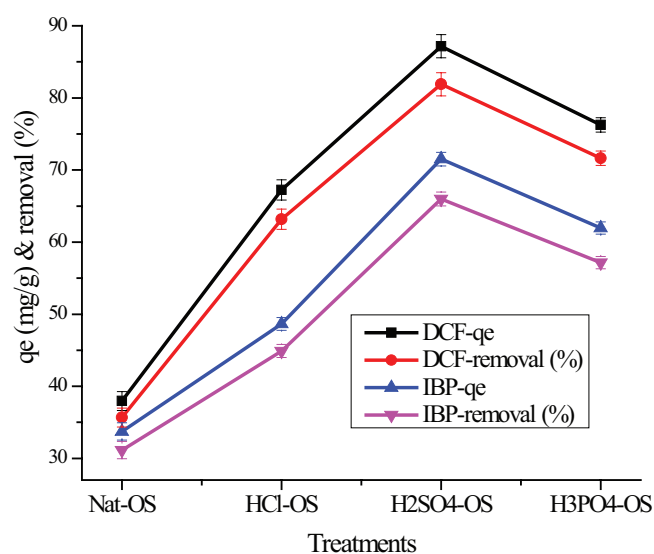


Fig. 7. Effect of acids pre-treatments on adsorption of (a) diclofenac (b) ibuprofen on onion skin activated with acids (adsorbent dose = 0.05 g, pH = 6.5, contact time = 4 h, initial concentration of drugs = 20 mg/L).

3.6. Equilibrium modeling

Freundlich and Langmuir adsorption isotherms were applied to describe the equilibrium relationships between sorbent and sorbate in solution. The Langmuir model assumes monolayer adsorption onto a surface containing a finite number of adsorption sites of uniform energies. The Langmuir isotherm predicts linear adsorption at low adsorption densities and maximum surface coverage [95]. The linear mathematical form of Langmuir is shown in Eq. (9):

$$\frac{1}{q_e} = \frac{1}{Q_0} + \frac{1}{bQ_0C_e} \quad (9)$$

where q_e (mg/g), C_e (mg/L), Q_0 (mg/g) and b (L/mg) represent the amount of dye adsorbed at equilibrium/unit mass of adsorbent, equilibrium dye concentration, maximum dye adsorbed per unit mass of adsorbent to form a monolayer at higher C_e values, respectively, and b is related to the energy of the adsorption.

The Freundlich isotherm exponential form is shown in Eq. (10) [96,97]:

$$q_e = K_F C_e^{1/n} \quad (10)$$

where K_F (mg/g) and n are the constants, and K_F represents the adsorption capacity/unit mass of adsorbent. The $1/n$ value reveals the favorability of adsorption and $1/n$ value > 1 indicates the favorable adsorption of adsorbate onto the adsorbent [62,76].

The Freundlich and Langmuir constants with R^2 values are shown in Table 1. The R^2 values were 0.1551, 0.4403, 0.6017 and 0.6586 (for DCF) and 0.0029, 0.5145, 0.9040 and 0.0291 (IBP) for Nat-OS, HCl-OS, H_2SO_4 -OS and H_3PO_4 -OS adsorbents, respectively. The HCl-OS, H_2SO_4 -OS and H_3PO_4 -OS adsorption capacities determined experimentally were in agreement with Freundlich isotherm, which is an indication that DCF and IBP followed Freundlich isotherm for adsorption onto OS adsorbents. The Freundlich isotherm explains adsorption onto heterogeneous surface. Stronger binding sites are occupied first and binding strength decreased with increasing the degree of site occupation. The Freundlich isotherm assumes that a monolayer sorption with a heterogeneous energetic distribution of active sites accompanied by interaction between adsorbed molecules. The value of $1/n > 1$ indicates that adsorption took place at high concentration. K_f is a measure of the degree or strength of adsorption, while $1/n$ is used as an indication whether adsorption remains constant or decreased with increasing adsorbate concentration [96,97].

3.7. Kinetic modeling

The pseudo-first-order and pseudo-second-order kinetic models were fitted to the experimental data [98,99]. The mathematical forms of pseudo-second-order kinetic model are shown in Eqs. (11) and (12), whereas pseudo-second-order kinetic model relations are shown in Eqs. (13) and (14), respectively:

$$\frac{dq}{dt} = k_1(q_e - q_t) \quad (11)$$

$$\log(q_e - q_t) = \log q_e - \frac{k_1}{2.303}t \quad (12)$$

where k_1 (min^{-1}), q_e (mg/g) and q (mg/g) are the rate constant, dye adsorbed at equilibrium, dye adsorbed at time t , respectively, and t is time. The k_1 was determined from the slope of plot $\log(q_e - q)$ vs. t .

$$\frac{dq}{dt} = k_2(q_e - q_t)^2 \quad (13)$$

$$\frac{t}{q_t} = \frac{1}{k_2 q_e^2} + \frac{t}{q_e} \quad (14)$$

where k_2 ($\text{g}^{-1}\text{min}^{-1}$) and q_e (mg/g) are the constant and adsorption capacity at equilibrium, which were determined from the slope and intercept of plot t/q_t vs. time. The kinetics data is presented in Table 2. The pseudo-first-order kinetic model seems inadequate to predict the experimental adsorption capacity of drugs onto OS. The calculated R^2 values in

case of pseudo-first-order were relatively low as compared with pseudo-second-order kinetic model. Moreover, the q_e experimental values were in agreement with calculated q_e values, which imply that pseudo-second-order kinetic model fitted well to the drugs adsorption onto OS adsorbents, which implies that the drugs adsorption followed the pseudo-second-order kinetic model and the adsorption rate coefficient is a function of contact time [98–102].

3.8. SEM and EDX studies

SEM is used to study the morphological and surface characteristics of the adsorbents. The surface morphologies of loaded and un-loaded Nat-OS and pre-treated were monitored by SEM. Fig. 8 represents the SEM images of Nat-OS (un-loaded), mineral acids pre-treated (un-loaded) and drugs loaded adsorbents. The SEM images show that the surface morphologies of Nat-OS, acids pre-treated un-loaded and drugs loaded OS were changed significantly. The fibrous texture was not prominent and the crystalline texture was clear of the OS adsorbents [103]. As a result of acids pre-treatments, the surface roughness was changed and fibrous texture was exposed. The effect on surface morphology was more prominent in case of H_2SO_4 and H_3PO_4 as compared with HCl, which indicates that leaching of impurities and rupture of surface cellulose was occurred as

Table 1

Comparison of Langmuir and Freundlich isotherms for the adsorption of diclofenac and ibuprofen on onion skin activated with acids

Drugs	Langmuir isotherm				Freundlich isotherm				
	Adsorbents	X_m (mg/g)	K_L (L/mg)	R^2	Experimental value q_{max} (mg/g)	$1/n$	K_f (mg/g)	R^2	q_e (mg/g)
DCF	Nat-OS	0.1552	0.0013	0.1552	69.0678	1.0145	2.0132	0.9815	62.8
	HCl-OS	0.4403	0.0094	0.4403	112.3042	1.4552	4.9968	0.9406	134.55
	H_2SO_4 -OS	0.6017	0.0108	0.6017	134.0035	0.9128	4.3984	0.9685	165.19
	H_3PO_4 -OS	0.6586	0.0088	0.6586	124.2572	0.8337	3.9994	0.9889	126.38
IBP	Nat-OS	714.285	0.0005	0.0029	41.6641	1.0707	4.1314	0.9244	50.9565
	HCl-OS	158.730	0.00660	0.5145	68.5933	0.8122	1.5591	0.9461	76.5596
	H_2SO_4 -OS	147.058	0.01808	0.904	91.99	0.7388	3.7402	0.9657	105.438
	H_3PO_4 -OS	34.3642	0.02920	0.0291	79.023	1.0575	1.2897	0.9241	78.7045

Table 2

Comparison between pseudo-first-order and pseudo-second-order kinetic parameters for the adsorption of diclofenac and ibuprofen on onion skin activated with acids

Drugs	Adsorbents	Pseudo-first-order			Pseudo-second-order			
		q_e (mg/g)	K_{lad} (min^{-1})	R^2	q_{exp} (mg/g)	q_e (mg/g)	K_{2ad} (mg/g min)	R^2
DCF	Nat-OS	13.54877	0.00083	0.6039	28.55	29.41176	0.001271	0.9982
	HCl-OS	17.46224	0.00039	0.5453	47.61	50	0.000874	0.998
	H_2SO_4 -OS	30.50001	0.00096	0.8377	68.42	73.52941	0.000763	0.9997
	H_3PO_4 -OS	19.85638	0.00069	0.3767	60.3	60.97561	0.000782	0.9951
IBP	Nat-OS	9.788136	0.0003	0.6039	21.45	19.56947	0.002425	0.9909
	HCl-OS	14.5278	0.00056	0.5453	36.41	37.17472	0.000583	0.9915
	H_2SO_4 -OS	18.27679	0.00065	0.8377	48.26	49.26108	0.000645	0.9957
	H_3PO_4 -OS	19.18669	0.00074	0.3767	43.18	46.08295	0.000268	0.9812

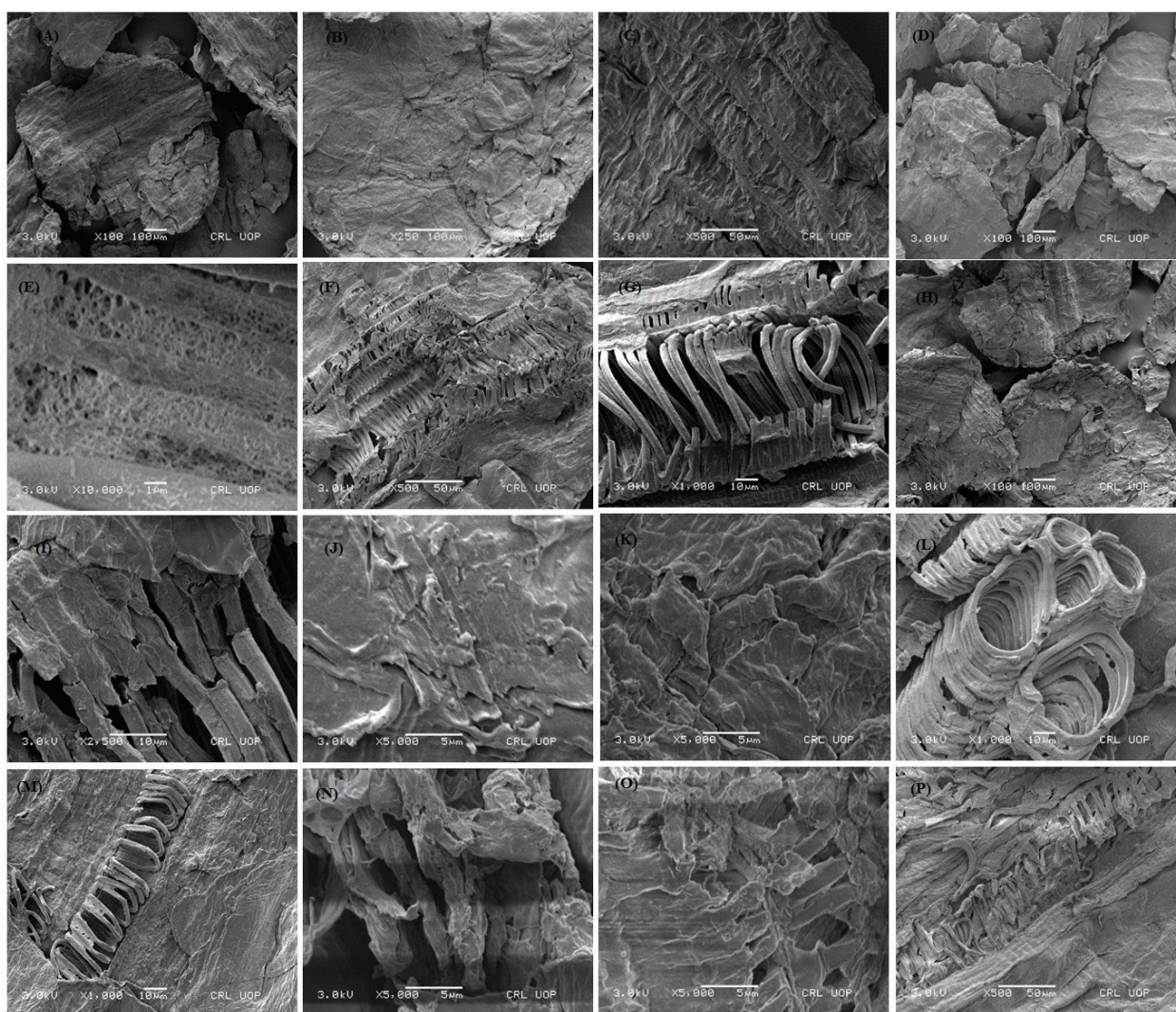


Fig. 8. (A–C) SEM images of un-loaded Nat-OS, (D, E) SEM image of HCl pre-treated OS without loading drugs, (F, G) SEM image of H_2SO_4 -OS without loading drugs, (H, I) SEM image of H_3PO_4 -OS without loading drugs, (J, K) SEM image of native and HCl-treated OS after loading of DCF, (L, M) SEM image of H_2SO_4 and H_3PO_4 -treated OS after loading of DCF and (N–P) SEM images of Nat-OS, HCl-OS, H_2SO_4 -OS after loading of ibuprofen.

a result of acids pre-treatments HCl and H_2SO_4 and H_3PO_4 . Previous studies also revealed that the physico-chemical treatment of the adsorbent changed the surface characteristics of the adsorbents and resultantly, adsorption of adsorbate also affected [91,92]. Pre-treatment changed the OS surface and the surface turned to porous structure as a result of acids pre-treatments. The mineral acid treatment leached the inorganic ions and adsorbent textural characteristics favored the adsorption [104]. EDX analysis was performed to determine the elemental composition of the adsorbents (Nat-OS, acids pre-treated and drugs loaded OS adsorbents) and results are shown in Fig. 9. Results showed that N, C, O, S, Ca, Zn, Si, Mg, Fe, Cl and Cu were present in un-loaded OS adsorbent. This composition correlates with reported composition of onion [105,106]. In acid pre-treated OS, the inorganic impurities were leached, which induced the roughness and grooves on the surface, which facilitates the adsorption of drugs. H_2SO_4 and H_3PO_4 acids

pre-treatments showed better mobilization of metal ions as compared with HCl. After adsorption of drugs, the peaks detected in un-loaded OS were disappeared and new peaks were appeared, which reveals the change in OS composition due to drugs adsorption.

4. Conclusions

OS was activated with HCl, H_2SO_4 and H_3PO_4 acids and resultant adsorbents were investigated for the adsorption of NSAIDs (DCF and IBP). The influence of process variables, that is, acids pre-treatments, pH, initial drugs concentrations, adsorbent dose and contact time were optimized for maximum adsorption of the drugs. The OS modification with H_2SO_4 enhanced the adsorption capacity up to 56% vs. Nat-OS. The optimum conditions of pH, adsorbent dosage and contact time were 6.5, 0.05 mg/g and 220 min, respectively. At optimum condition, the DCF and IBP adsorptions

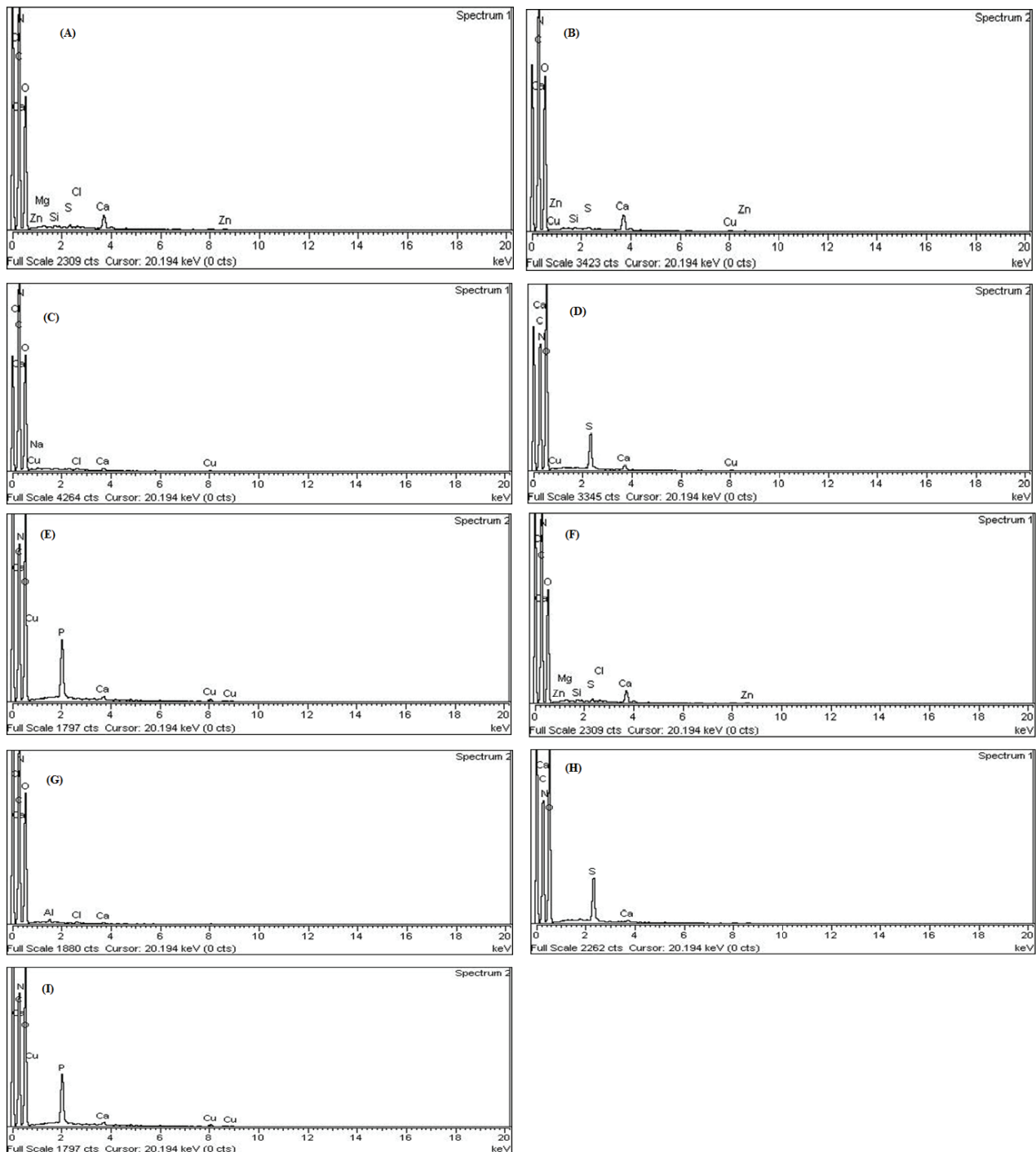


Fig. 9. (A, B) EDX spectra of native onion skin, (C–E) EDX spectra of acids pre-treated onion skin, (F–I) EDX spectra of drugs loaded native, HCl, H_2SO_4 and H_3PO_4 pre-treated onion skin.

were 134.003 and 91.99 mg/g, respectively, which were 81.90% and 65.99% removal of the initial concentrations. H_2SO_4 -OS showed maximum drugs adsorption followed by H_3PO_4 -OS, HCl-OS and Nat-OS. The drugs adsorption onto OS adsorbents followed Freundlich isotherm and pseudo-second-order kinetic model. Results revealed that the OS is an efficient adsorbent and could possibly be used for the remediation of pharmaceutical drugs from wastewater.

References

- [1] K.E. Arnold, A.B. Boxall, A.R. Brown, R.J. Cuthbert, S. Gaw, T.H. Hutchinson, S. Jobling, J.C. Madden, C.D. Metcalfe, V. Naidoo, Assessing the exposure risk and impacts of pharmaceuticals in the environment on individuals and ecosystems, *Biol. Lett.*, 9 (2013) 20130492.
- [2] G. McEneff, L. Barron, B. Kelleher, B. Paull, B. Quinn, A year-long study of the spatial occurrence and relative distribution of pharmaceutical residues in sewage effluent, receiving marine

- waters and marine bivalves, *Sci. Total Environ.*, 476 (2014) 317–326.
- [3] K. Dutta, M.-Y. Lee, W.W.-P. Lai, C.H. Lee, A.Y.-C. Lin, C.-F. Lin, J.-G. Lin, Removal of pharmaceuticals and organic matter from municipal wastewater using two-stage anaerobic fluidized membrane bioreactor, *Bioresour. Technol.*, 165 (2014) 42–49.
- [4] C.G. Daughton, Pharmaceuticals in the environment: sources and their management, *Compr. Anal. Chem.*, 50 (2007) 1–58.
- [5] S. Mompelat, B. Le Bot, O. Thomas, Occurrence and fate of pharmaceutical products and by-products, from resource to drinking water, *Environ. Int.*, 35 (2009) 803–814.
- [6] D.Q. Zhang, T. Hua, R.M. Gersberg, J. Zhu, W.J. Ng, S.K. Tan, Fate of diclofenac in wetland mesocosms planted with *Scirpus validus*, *Ecol. Eng.*, 49 (2012) 59–64.
- [7] A. Hallare, H.-R. Köhler, R. Triebskorn, Developmental toxicity and stress protein responses in zebrafish embryos after exposure to diclofenac and its solvent, DMSO, *Chemosphere*, 56 (2004) 659–666.
- [8] M. Schriks, M.B. Heringa, M.M. van der Kooij, P. de Voogt, A.P. van Wezel, Toxicological relevance of emerging contaminants for drinking water quality, *Water Res.*, 44 (2010) 461–476.
- [9] V. Prakash, M.C. Bishwakarma, A. Chaudhary, R. Cuthbert, R. Dave, M. Kulkarni, S. Kumar, K. Paudel, S. Ranade, R. Shringarpure, The population decline of *Gyps* vultures in India and Nepal has slowed since veterinary use of diclofenac was banned, *PLoS One*, 7 (2012) e49118.
- [10] I.A. Vasiliadou, R. Molina, F. Martínez, J.A. Melero, Biological removal of pharmaceutical and personal care products by a mixed microbial culture: sorption, desorption and biodegradation, *Biochem. Eng. J.*, 81 (2013) 108–119.
- [11] A. Babarinde, K. Ogundipe, K.T. Sangosanya, B.D. Akintola, A.-O. Elizabeth Hassan, Comparative study on the biosorption of Pb(II), Cd(II) and Zn(II) using Lemon grass (*Cymbopogon citratus*): kinetics, isotherms and thermodynamics, *Chem. Int.*, 2 (2016) 89–102.
- [12] A. Babarinde, G.O. Onyiaocha, Equilibrium sorption of divalent metal ions onto groundnut (*Arachis hypogaea*) shell: kinetics, isotherm and thermodynamics, *Chem. Int.*, 2 (2016) 37–46.
- [13] M. Iqbal, R.A. Khera, Adsorption of copper and lead in single and binary metal system onto *Fumaria indica* biomass, *Chem. Int.*, 1 (2015) 157b–163b.
- [14] M.A. Jamal, M. Muneer, M. Iqbal, Photo-degradation of monoazo dye blue 13 using advanced oxidation process, *Chem. Int.*, 1 (2015) 12–16.
- [15] K. Qureshi, M. Ahmad, I. Bhatti, M. Iqbal, A. Khan, Cytotoxicity reduction of wastewater treated by advanced oxidation process, *Chem. Int.*, 1 (2015) 53–59.
- [16] G.R. Boyd, H. Reemtsma, D.A. Grimm, S. Mitra, Pharmaceuticals and personal care products (PPCPs) in surface and treated waters of Louisiana, USA and Ontario, Canada, *Sci. Total Environ.*, 311 (2003) 135–149.
- [17] T.D. Bonilla, K. Nowosielski, M. Cuvelier, A. Hartz, M. Green, N. Esiobu, D.S. McCorquodale, J.M. Fleisher, A. Rogerson, Prevalence and distribution of fecal indicator organisms in South Florida beach sand and preliminary assessment of health effects associated with beach sand exposure, *Marine Pollut. Bull.*, 54 (2007) 1472–1482.
- [18] V.J. Pereira, K.G. Linden, H.S. Weinberg, Evaluation of UV irradiation for photolytic and oxidative degradation of pharmaceutical compounds in water, *Water Res.*, 41 (2007) 4413–4423.
- [19] F.J. Beltrán, A. Aguinaco, J.F. García-Araya, Kinetic modelling of TOC removal in the photocatalytic ozonation of diclofenac aqueous solutions, *Appl. Catal., B*, 100 (2010) 289–298.
- [20] E. Nie, M. Yang, D. Wang, X. Yang, X. Luo, Z. Zheng, Degradation of diclofenac by ultrasonic irradiation: kinetic studies and degradation pathways, *Chemosphere*, 113 (2014) 165–170.
- [21] I. González-Mariño, J.B. Quintana, I. Rodríguez, N. Sánchez-Méndez, R. Cela, Transformation of cocaine during water chlorination, *Anal. Bioanal. Chem.*, 404 (2012) 3135–3144.
- [22] S. Nouren, H.N. Bhatti, M. Iqbal, I. Bibi, S. Kamal, S. Sadaf, M. Sultan, A. Kausar, Y. Safa, By-product identification and phytotoxicity of biodegraded Direct Yellow 4 dye, *Chemosphere*, 169 (2017) 474–484.
- [23] M. Mushtaq, H.N. Bhatti, M. Iqbal, S. Noreen, *Eriobotrya japonica* seed biocomposite efficiency for copper adsorption: isotherms, kinetics, thermodynamic and desorption studies, *J. Environ. Manage.*, 176 (2016) 21–33.
- [24] R. Nadeem, Q. Manzoor, M. Iqbal, J. Nisar, Biosorption of Pb (II) onto immobilized and native *Mangifera indica* waste biomass, *J. Ind. Eng. Chem.*, 35 (2016) 185–194.
- [25] A. Rashid, H.N. Bhatti, M. Iqbal, S. Noreen, Fungal biomass composite with bentonite efficiency for nickel and zinc adsorption: a mechanistic study, *Ecol. Eng.*, 91 (2016) 459–471.
- [26] S. Shoukat, H.N. Bhatti, M. Iqbal, S. Noreen, Mango stone biocomposite preparation and application for crystal violet adsorption: a mechanistic study, *Micropor. Mesopor. Mater.*, 239 (2017) 180–189.
- [27] M.A. Tahir, H.N. Bhatti, M. Iqbal, Solar Red and Brittle Blue direct dyes adsorption onto *Eucalyptus angophoroides* bark: equilibrium, kinetics and thermodynamic studies, *J. Environ. Chem. Eng.*, 4 (2016) 2431–2439.
- [28] N.K. Benabdallah, D. Harrache, A. Mir, M. de la Guardia, F.-Z. Benhachem, Bioaccumulation of trace metals by red alga *Corallina elongata* in the coast of Beni Saf, west coast, Algeria, *Chem. Int.*, 3 (2017) 220–231.
- [29] A.M. Engida, B.S. Chandravanshi, Assessment of heavy metals in tobacco of cigarettes commonly sold in Ethiopia, *Chem. Int.*, 3 (2017) 213–219.
- [30] S. Isah, A.A. Oshodi, V.N. Atasi, Physicochemical properties of cross linked acha (*digitaria exilis*) starch with citric acid, *Chem. Int.*, 3 (2017) 150–157.
- [31] S. Jafarinejad, Control and treatment of sulfur compounds specially sulfur oxides (SOx) emissions from the petroleum industry: a review, *Chem. Int.*, 2 (2016) 242–253.
- [32] S. Jafarinejad, Recent developments in the application of sequencing batch reactor (SBR) technology for the petroleum industry wastewater treatment, *Chem. Int.*, 3 (2017) 241–250.
- [33] S. Jafarinejad, Activated sludge combined with powdered activated carbon (PACT process) for the petroleum industry wastewater treatment: a review, *Chem. Int.*, 3 (2017) 268–277.
- [34] K. Legrouiri, E. Khouya, H. Hannache, M. El Hartti, M. Ezzine, R. Naslain, Activated carbon from molasses efficiency for Cr(VI), Pb(II) and Cu(II) adsorption: a mechanistic study, *Chem. Int.*, 3 (2017) 301–310.
- [35] A.O. Majolagbe, A.A. Adeyi, O. Osibanjo, Vulnerability assessment of groundwater pollution in the vicinity of an active dumpsite (Olusosun), Lagos, Nigeria, *Chem. Int.*, 2 (2016) 232–241.
- [36] A.O. Majolagbe, A.A. Adeyi, O. Osibanjo, A.O. Adams, O.O. Ojuri, Pollution vulnerability and health risk assessment of groundwater around an engineering landfill in Lagos, Nigeria, *Chem. Int.*, 3 (2017) 58–68.
- [37] K.D. Ogundipe, A. Babarinde, Comparative study on batch equilibrium biosorption of Cd(II), Pb(II) and Zn(II) using plantain (*Musa paradisiaca*) flower: kinetics, isotherm, and thermodynamics, *Chem. Int.*, 3 (2017) 135–149.
- [38] U.C. Peter, U. Chinedu, Model prediction for constant area, variable pressure drop in orifice plate characteristics in flow system, *Chem. Int.*, 2 (2016) 80–88.
- [39] V.R. Remya, V.K. Abitha, P.S. Rajput, A.V. Rane, A. Dutta, Silver nanoparticles green synthesis: a mini review, *Chem. Int.*, 3 (2017) 165–171.
- [40] A. Shindy, Problems and solutions in colors, dyes and pigments chemistry: a review, *Chem. Int.*, 3 (2017) 97–105.
- [41] H. Shindy, Basics in colors, dyes and pigments chemistry: a review, *Chem. Int.*, 2 (2016) 29–36.
- [42] C. Ukpaka, Development of model for bioremediation of crude oil using moringa extract, *Chem. Int.*, 2 (2016) 19–28.
- [43] C. Ukpaka, Predictive model on the effect of restrictor on transfer function parameters on pneumatic control system, *Chem. Int.*, 2 (2016) 128–135.
- [44] C. Ukpaka, Empirical model approach for the evaluation of pH and conductivity on pollutant diffusion in soil environment, *Chem. Int.*, 2 (2016) 267–278.

- [45] C. Ukpaka, BTX degradation: the concept of microbial integration, *Chem. Int.*, 3 (2016) 8–18.
- [46] C. Ukpaka, S.N.-A. Adaobi, C. Ukpaka, Development and evaluation of trans-amadi groundwater parameters: the integration of finite element techniques, *Chem. Int.*, 3 (2017) 306–317.
- [47] C. Ukpaka, T. Izonowei, Model prediction on the reliability of fixed bed reactor for ammonia production, *Chem. Int.*, 3 (2017) 46–57.
- [48] C. Ukpaka, C. Ukpaka, Characteristics of groundwater in Port-Harcourt local Government area, *Chem. Int.*, 2 (2016) 136–144.
- [49] C.P. Ukpaka, F.U. Igwe, Modeling of the velocity profile of a bioreactor: the concept of biochemical process, *Chem. Int.*, 3 (2017) 258–267.
- [50] S. Adeel, M. Usman, W. Haider, M. Saeed, M. Muneer, M. Ali, Dyeing of gamma irradiated cotton using Direct Yellow 12 and Direct Yellow 27: improvement in colour strength and fastness properties, *Cellulose*, 22 (2015) 2095–2105.
- [51] M. Ajmal, S. Adeel, M. Azeem, M. Zuber, N. Akhtar, N. Iqbal, Modulation of pomegranate peel colourant characteristics for textile dyeing using high energy radiations, *Ind. Crop. Product*, 58 (2014) 188–193.
- [52] F. Bouatay, N. Meksi, S. Adeel, F. Salah, F. Mhenni, Dyeing behavior of the cellulosic and jute fibers with cationic dyes: process development and optimization using statistical analysis, *J. Nat. Fibers*, 13 (2016) 423–436.
- [53] M. Muneer, S. Adeel, S. Ayub, M. Zuber, F. Ur-Rehman, M. Kanjal, M. Iqbal, M. Kamran, Dyeing behaviour of microwave assisted surface modified polyester fabric using disperse orange 25: improvement in colour strength and fastness properties, *Oxid. Commun.*, 39 (2016) 1430–1439.
- [54] C. Saka, Ö. Şahin, M. Celik, The removal of methylene blue from aqueous solutions by using microwave heating and pre-boiling treated onion skins as a new adsorbent, *Energy Sources Part A*, 34 (2012) 1577–1590.
- [55] A. Sasmaz, I.M. Dogan, M. Sasmaz, Removal of Cr, Ni and Co in the water of chromium mining areas by using *Lemna gibba* L. and *Lemna minor* L., *Water Environ. J.*, 30 (2016) 235–242.
- [56] M. Sasmaz, B. Akgül, D. Yıldırım, A. Sasmaz, Bioaccumulation of thallium by the wild plants grown in soils of mining area, *Int. J. Phytoremed.*, 18 (2016) 1164–1170.
- [57] M. Sasmaz, B. Akgül, D. Yıldırım, A. Sasmaz, Mercury uptake and phytotoxicity in terrestrial plants grown naturally in the Gumuskoy (Kutahya) mining area, Turkey, *Int. J. Phytoremed.*, 18 (2016) 69–76.
- [58] M. Sasmaz, E.I.A. Topal, E. Obek, A. Sasmaz, The potential of *Lemna gibba* L. and *Lemna minor* L. to remove Cu, Pb, Zn, and As in gallery water in a mining area in Keban, Turkey, *J. Environ. Manage.*, 163 (2015) 246–253.
- [59] K.M. Khokhar, Growing Onion in Pakistan, 2005. Available at: <https://www.linkedin.com/pulse/growing-onion-pakistan-dr-khalid-mahmud-khokhar>.
- [60] FAOSTAT, Agriculture Organization of the United Nations, FAO, 2011, Available at: <http://faostat3.fao.org/faostat-gateway/go/to/download/Q/QC/S> (Accessed 20 August, 2015).
- [61] C. Saka, Ö. Sahin, Removal of methylene blue from aqueous solutions by using cold plasma-and formaldehyde-treated onion skins, *Color. Technol.*, 127 (2011) 246–255.
- [62] Q. Manzoor, R. Nadeem, M. Iqbal, R. Saeed, T.M. Ansari, Organic acids pretreatment effect on *Rosa bourbonia* phyto-biomass for removal of Pb (II) and Cu (II) from aqueous media, *Bioresour. Technol.*, 132 (2013) 446–452.
- [63] H.N. Bhatti, I.I. Bajwa, M.A. Hanif, I.H. Bukhari, Removal of lead and cobalt using lignocellulosic fiber derived from *Citrus reticulata* waste biomass, *Korean J. Chem. Eng.*, 27 (2010) 218–227.
- [64] S. Bajpai, M. Bhowmik, Adsorption of diclofenac sodium from aqueous solution using polyaniline as a potential sorbent. I. Kinetic studies, *J. Appl. Polym. Sci.*, 117 (2010) 3615–3622.
- [65] T.X. Bui, H. Choi, Adsorptive removal of selected pharmaceuticals by mesoporous silica SBA-15, *J. Hazard. Mater.*, 168 (2009) 602–608.
- [66] M. Antunes, V.I. Esteves, R. Guégan, J.S. Crespo, A.N. Fernandes, M. Giovanela, Removal of diclofenac sodium from aqueous solution by Isabel grape bagasse, *Chem. Eng. J.*, 192 (2012) 114–121.
- [67] R. Baccar, M. Sarrà, J. Bouzid, M. Feki, P. Blánquez, Removal of pharmaceutical compounds by activated carbon prepared from agricultural by-product, *Chem. Eng. J.*, 211 (2012) 310–317.
- [68] R. Gong, Y. Ding, H. Liu, Q. Chen, Z. Liu, Lead biosorption and desorption by intact and pretreated *Spirulina maxima* biomass, *Chemosphere*, 58 (2005) 125–130.
- [69] N. Tahir, H.N. Bhatti, M. Iqbal, S. Noreen, Biopolymers composites with peanut hull waste biomass and application for Crystal Violet adsorption, *Int. J. Biol. Macromol.*, 94 (2016) 210–220.
- [70] A.E. Ofomaja, Y.-S. Ho, Equilibrium sorption of anionic dye from aqueous solution by palm kernel fibre as sorbent, *Dyes Pigm.*, 74 (2007) 60–66.
- [71] A. Shukla, Y.-H. Zhang, P. Dubey, J. Margrave, S.S. Shukla, The role of sawdust in the removal of unwanted materials from water, *J. Hazard. Mater.*, 95 (2002) 137–152.
- [72] H. Naeem, H.N. Bhatti, S. Sadaf, M. Iqbal, Uranium remediation using modified *Vigna radiata* waste biomass, *Appl. Radiat. Isot.*, 123 (2017) 94–101.
- [73] N. Tewari, P. Vasudevan, B. Guha, Study on biosorption of Cr (VI) by *Mucor hiemalis*, *Biochem. Eng. J.*, 23 (2005) 185–192.
- [74] K.A. Shroff, V.K. Vaidya, Kinetics and equilibrium studies on biosorption of nickel from aqueous solution by dead fungal biomass of *Mucor hiemalis*, *Chem. Eng. J.*, 171 (2011) 1234–1245.
- [75] M. Iqbal, N. Iqbal, I.A. Bhatti, N. Ahmad, M. Zahid, Response surface methodology application in optimization of cadmium adsorption by shoe waste: a good option of waste mitigation by waste, *Ecol. Eng.*, 88 (2016) 265–275.
- [76] I. Ullah, R. Nadeem, M. Iqbal, Q. Manzoor, Biosorption of chromium onto native and immobilized sugarcane bagasse waste biomass, *Ecol. Eng.*, 60 (2013) 99–107.
- [77] H.N. Bhatti, A. Jabeen, M. Iqbal, S. Noreen, Z. Naseem, Adsorptive behavior of rice bran-based composites for malachite green dye: isotherm, kinetic and thermodynamic studies, *J. Mol. Liq.*, 237 (2017) 322–333.
- [78] H.N. Bhatti, Q. Zaman, A. Kausar, S. Noreen, M. Iqbal, Efficient remediation of Zr(IV) using citrus peel waste biomass: kinetic, equilibrium and thermodynamic studies, *Ecol. Eng.*, 95 (2016) 216–228.
- [79] H.M. Clark, C.C. Alves, A.S. Franca, L.S. Oliveira, Evaluation of the performance of an agricultural residue-based activated carbon aiming at removal of phenylalanine from aqueous solutions, *LWT – Food Sci. Technol.*, 49 (2012) 155–161.
- [80] G. Moussavi, B. Barikbin, Biosorption of chromium (VI) from industrial wastewater onto pistachio hull waste biomass, *Chem. Eng. J.*, 162 (2010) 893–900.
- [81] J. Iqbal, F. Cecil, K. Ahmad, M. Iqbal, M. Mushtaq, M. Naeem, T. Bokhari, Kinetic study of Cr (III) and Cr (VI) biosorption using *Rosa damascena* phyto-mass: a rose waste biomass, *Asian J. Chem.*, 25 (2013) 2099–2103.
- [82] S. Kanchana, J. Jeyanthi, R.D. Kumar, Equilibrium and kinetic studies on biosorption of chromium (VI) on to *Chlorella* species, *Eur. J. Sci. Res.*, 63 (2011) 255–262.
- [83] L. Lakshmanraj, A. Gurusamy, M. Gobinath, R. Chandramohan, Studies on the biosorption of hexavalent chromium from aqueous solutions by using boiled mucilaginous seeds of *Ocimum americanum*, *J. Hazard. Mater.*, 169 (2009) 1141–1145.
- [84] S. Ghosh, A. Mondal, A. Paul, Hexavalent chromium biosorption by dried biomass of *Aspergillus niger* NUA101 isolated from Indian ultramafic complex, *Afr. J. Microbiol. Res.*, 9 (2015) 220–229.
- [85] J.R. Memon, S.Q. Memon, M.I. Bhangar, A. El-Turki, K.R. Hallam, G.C. Allen, Banana peel: a green and economical sorbent for the selective removal of Cr (VI) from industrial wastewater, *Colloids Surf., B*, 70 (2009) 232–237.
- [86] A.P. Marín, M. Aguilar, V. Meseguer, J. Ortuno, J. Sáez, M. Lloréns, Biosorption of chromium (III) by orange (*Citrus cinensis*) waste: batch and continuous studies, *Chem. Eng. J.*, 155 (2009) 199–206.

- [87] X.S. Wang, Z.Z. Li, S.R. Tao, Removal of chromium (VI) from aqueous solution using walnut hull, *J. Environ. Manage.*, 90 (2009) 721–729.
- [88] R. Marandi, Biosorption of hexavalent chromium from aqueous solution by dead fungal biomass of *Phanerochaete chrysosporium*: batch and fixed bed studies, *Can. J. Chem. Eng. Technol.*, 2 (2011) 8–22.
- [89] M. Akram, H.N. Bhatti, M. Iqbal, S. Noreen, S. Sadaf, Biocomposite efficiency for Cr(VI) adsorption: kinetic, equilibrium and thermodynamics studies, *J. Environ. Chem. Eng.*, 5 (2017) 400–411.
- [90] M.N. Zafar, A. Parveen, R. Nadeem, A pretreated green biosorbent based on neem leaves biomass for the removal of lead from wastewater, *Desal. Wat. Treat.*, 51 (2013) 4459–4466.
- [91] A. Bhatnagar, M. Sillanpää, A. Witek-Krowiak, Agricultural waste peels as versatile biomass for water purification – a review, *Chem. Eng. J.*, 270 (2015) 244–271.
- [92] H.N. Bhatti, R. Khalid, M.A. Hanif, Dynamic biosorption of Zn (II) and Cu (II) using pretreated *Rosa gruss an teplitz* (red rose) distillation sludge, *Chem. Eng. J.*, 148 (2009) 434–443.
- [93] H. Guedidi, L. Reinert, J.-M. Lévêque, Y. Soneda, N. Bellakhal, L. Duclaux, The effects of the surface oxidation of activated carbon, the solution pH and the temperature on adsorption of ibuprofen, *Carbon*, 54 (2013) 432–443.
- [94] M.K. Toor, Enhancing Adsorption Capacity of Bentonite for Dye Removal: Physicochemical Modification and Characterization, Thesis, School of Chemical Engineering, The University of Adelaide, 2011.
- [95] I. Langmuir, The adsorption of gases on plane surfaces of glass, mica and platinum, *J. Am. Chem. Soc.*, 40 (1918) 1361–1403.
- [96] H. Freundlich, Over the adsorption in solution, *J. Phys. Chem.*, 57 (1906) 1100–1107.
- [97] H. Freundlich, A. Seal, Ueber einige Eigenschaften des Rhodanions, *Colloid Polym. Sci.*, 11 (1912) 257–263.
- [98] Y. Ho, G. McKay, The sorption of lead (II) ions on peat, *Water Res.*, 33 (1999) 578–584.
- [99] Y.-S. Ho, Review of second-order models for adsorption systems, *J. Hazard. Mater.*, 136 (2006) 681–689.
- [100] M. Haerifar, S. Azizian, Fractal-like adsorption kinetics at the solid/solution interface, *J. Phys. Chem. C*, 116 (2012) 13111–13119.
- [101] M.J. Haas, A.J. McAloon, W.C. Yee, T.A. Foglia, A process model to estimate biodiesel production costs, *Bioresour. Technol.*, 97 (2006) 671–678.
- [102] Y. Ho, G. McKay, Competitive sorption of copper and nickel ions from aqueous solution using peat, *Adsorption*, 5 (1999) 409–417.
- [103] M.C. Ribas, M.A. Adebayo, L.D. Prola, E.C. Lima, R. Cataluña, L.A. Feris, M. Puchana-Rosero, F.M. Machado, F.A. Pavan, T. Calvete, Comparison of a homemade cocoa shell activated carbon with commercial activated carbon for the removal of reactive violet 5 dye from aqueous solutions, *Chem. Eng. J.*, 248 (2014) 315–326.
- [104] D.C. dos Santos, M.A. Adebayo, S.d.F.P. Pereira, L.D.T. Prola, R. Cataluña, E.C. Lima, C. Saucier, C.R. Gally, F.M. Machado, New carbon composite adsorbents for the removal of textile dyes from aqueous solutions: kinetic, equilibrium, and thermodynamic studies, *Korean J. Chem. Eng.*, 31 (2014) 1470–1479.
- [105] F. Golubev, N. Golubkina, Y.N. Gorbunov, Mineral composition of wild onions and their nutritional value, *Appl. Biochem. Microbiol.*, 39 (2003) 532–535.
- [106] N. Nnaji, C. Okoye, N. Obi-Egbedi, M. Ezeokonkwo, J. Ani, Spectroscopic characterization of red onion skin tannin and its use as alternative aluminium corrosion inhibitor in hydrochloric acid solutions, *Int. J. Electrochem. Sci.*, 8 (2013) 1735–1758.